

Article

Refining the Performance of mid-IR CPA Laser Systems Based on Fe-Doped Chalcogenides for Nonlinear Photonics

Andrey Pushkin and Fedor Potemkin * 

Faculty of Physics, Lomonosov Moscow State University, 119991 Moscow, Russia; av.pushkin@physics.msu.ru

* Correspondence: potemkin@physics.msu.ru

Abstract: The chirped pulse amplification (CPA) systems based on transition-metal-ion-doped chalcogenide crystals are promising powerful ultrafast laser sources providing access to sub-TW laser pulses in the mid-IR region, which are highly relevant for essential scientific and technological tasks, including high-field physics and attosecond science. The only way to obtain high-peak power few-cycle pulses is through efficient laser amplification, maintaining the gain bandwidth ultrabroad. In this paper, we report on the approaches for mid-IR broadband laser pulse energy scaling and the broadening of the gain bandwidth of iron-doped chalcogenide crystals. The multi-pass chirped pulse amplification in the Fe:ZnSe crystal with 100 mJ level nanosecond optical pumping provided more than 10 mJ of output energy at 4.6 μm . The broadband amplification in the Fe:ZnS crystal in the vicinity of 3.7 μm supports a gain band of more than 300 nm (FWHM). Spectral synthesis combining Fe:ZnSe and Fe:CdSe gain media allows the increase in the gain band (~500 nm (FWHM)) compared to using a single active element, thus opening the route to direct few-cycle laser pulse generation in the prospective mid-IR spectral range. The features of the nonlinear response of carbon nanotubes in the mid-IR range are investigated, including photoinduced absorption under 4.6 μm excitation. The study intends to expand the capabilities and improve the output characteristics of high-power mid-IR laser systems.

Keywords: mid-IR photonics; femtosecond; chalcogenides; chirped pulse amplification; spectral synthesis; low-dimensional nonlinear materials



Citation: Pushkin, A.; Potemkin, F. Refining the Performance of mid-IR CPA Laser Systems Based on Fe-Doped Chalcogenides for Nonlinear Photonics. *Photonics* **2023**, *10*, 1375. <https://doi.org/10.3390/photronics10121375>

Received: 22 November 2023

Revised: 7 December 2023

Accepted: 11 December 2023

Published: 14 December 2023



Copyright: © 2023 by the authors. Licensee MDPI, Basel, Switzerland. This article is an open access article distributed under the terms and conditions of the Creative Commons Attribution (CC BY) license (<https://creativecommons.org/licenses/by/4.0/>).

1. Introduction

In recent years, there has been a rapid development of ultrafast sources operating in the mid-infrared (mid-IR) spectral range, driven by their relevance for various applications [1]. The unique spectral and material properties of the gain media based on chalcogenides doped with transition metal ions, which have been developed over the past three decades [2], provided new possibilities and have gained prominence for their application in molecular and gas spectroscopy in the mid-IR range, which is often referred to as the “molecular fingerprints” region. The demand for high-intensity laser pulse sources has increased for the generation of high-field terahertz (up to GV/cm), extreme ultraviolet (EUV), and X-ray radiations through the nonperturbative regime of laser–matter interaction, leading to high harmonic and attosecond pulse generation [3–5]. This area of research was recently recognized by being awarded a Nobel Prize [6].

Chalcogenide crystals doped with iron ions offer exceptional possibilities for generating and amplifying laser pulses in the mid-IR range, spanning from 3.5 μm to 8 μm in various crystal hosts. The most prominent representatives of this group of active media are Fe:ZnSe, with a gain bandwidth spreading over 3.7–5.1 μm [7] and Fe:ZnS, tunable in the region of 3.4–4.2 μm [8]. In the longer wavelength range, Fe:CdSe and Fe:CdTe have demonstrated pulse generation at wavelengths of 4.6–6.1 μm and 5.1–6.3 μm , respectively. The shift of absorption and emission bands to longer wavelengths is achievable in $(A^2B^2)C^4$ compounds, particularly by introducing Mn or Mg ions to the ZnSe and CdTe lattice. This

enables controlled alterations of their laser properties. While these compounds are simpler to grow compared to pure selenide and sulfide crystals, their thermal properties are inferior, limiting their use for high average power generation.

For applications requiring high-intensity laser radiation, chirped pulse amplification (CPA) systems are indispensable. Chalcogenides doped with iron and chromium ions present remarkable prospects for generating broadband laser pulses with mJ level output energy. Unlike laser sources based on optical parametric chirped pulse amplification (OPCPA), conventional CPA systems do not demand picosecond-duration pumping pulses and exceptionally high beam quality. However, CPA systems require pumping lasers in the mid-IR range operating in a repetitively pulsed regime, which are not widely commercially available and are a great challenge to develop to date [9,10].

Previously, we demonstrated the potential of this approach using the Fe:ZnSe crystal with nanosecond optical pumping, implemented as a CPA system with an output energy of 3.5 mJ and 150 fs pulses at 4.4 μm [11]. Prior to that, such media were studied for generating long microsecond and nanosecond pulses, as well as continuous-wave radiation [12]. The use of a heavier CdSe host material allowed for shifting the gain bandwidth closer to 5 μm and obtaining pulses with an energy of approximately 1 mJ in a similar setup [13]. The approaches proposed by our scientific group laid the basis for the development of CPA systems based on Cr:ZnS/Se crystals with parametric seed and multi-pass amplification in a chalcogenide crystal pumped with nanosecond pulses [14,15]. At the same time, approaches for scaling the energy of pulses at a high repetition rate obtained from a Cr:ZnS chirped pulse oscillator in a continuous-wave pumped crystal have been introduced [16]. The consideration of Fe:ZnSe crystal pumping with long microsecond pulses at a wavelength of 3 μm with a high repetition rate is noteworthy [17]. The simplification of the pumping setup is offset by the complexity of the rest of the system, including the requirement to cool the active element in a helium cryostat, the suppression of amplified spontaneous emission (ASE) through the application of high-quality antireflection coatings on the crystal, and the use of an optical insulator in the mid-IR range, making such setup much more intricate and costly.

To broaden the application scope of such laser sources, the flexible control of its output parameters over a wide range is desired. This encompasses the ability for energy scaling, the shortening of pulse duration, and the tuning of the wavelength.

Energy scaling possibilities are associated with active investigations of crystals doped with iron ions that amplify their properties. For instance, the amplification characteristics of cryogenically cooled Fe:ZnSe were studied in the continuous-wave operation regime [18]. In the pulsed regime for a broadband laser pulse, research was conducted by our scientific group [19]. Further advancements in amplification can be achieved through the exploration of crystals with diverse properties, specifically the doping profile, which impacts the lifetime of the upper level and the position of the gain spectrum. The lack of information about the gain properties can potentially limit the controllability of the output laser parameters in such systems, such as increasing the laser pulse energy while maintaining a broadband gain spectrum.

Wide spectrum tunability can be achieved using various crystal hosts. In crystals with heavy ions, the gain spectrum shifts to a longer wavelength region. The amplification spectra of iron-doped chalcogenide crystals cover the spectral range from 3.5 μm to 8 μm . A promising approach for broadening the spectrum during amplification is spectral synthesis, a method developed for parametric sources that entails using several laser media to amplify radiation in various adjacent (overlapping) parts of the spectrum [20].

The mid-IR photonics component base is challenging to access. Low-dimensional carbon materials, such as graphene and nanotubes, are promising for the development of novel photonic devices due to the fact that they possess properties that are not characteristic of bulk materials. The saturable absorption of graphene and carbon nanotubes has been actively utilized to implement Q-switching and the mode-locking process in lasers [21]. Although semiconductor saturable mirrors (SESAMs) are employed for the mode-locking

process in the near-IR range, their optical properties do not yet allow for their extension into the long-wavelength spectral region beyond 3 μm . Carbon nanotubes, graphene, and other structures have shown promise in this range, but their properties are still poorly understood in the mid-IR. For instance, using graphene, we implemented, for the first time, ultrashort laser pulse generation in a Fe:ZnSe laser [22].

In this paper, we present several promising methods for controlling the parameters of pulses in the mid-IR range obtained in the CPA system based on iron-ion-doped chalcogenide crystals. These methods include increasing the output energy by multiplying the amplifier stages, wavelength tuning through the use of diverse crystal hosts, and spectral synthesis. Additionally, we discuss the potential of carbon nanotubes for the development of photonic devices in the mid-IR spectral range.

2. Energy Scaling of the Fe:ZnSe Multi-Pass Amplifier

The Fe:ZnSe crystal has demonstrated impressive results in both continuous-wave and pulsed regimes with microsecond or nanosecond durations [23,24]. This crystal exhibits an ultrabroad gain bandwidth in the mid-IR range, with a spectrum width of more than 1 μm at room temperature, potentially enabling the amplification of almost 50 fs pulses. Based on these features, we designed a CPA system (Figure 1) with an output spectrum width of about 220 nm (FWHM) at a central wavelength of 4.4 μm , achieving 3.5 mJ of output energy. The laser pulse was reshaped in a stretcher with an output pulse duration of 230 ps [11]. The complexity of the energy scaling procedure is associated with the low saturation fluence of the Fe:ZnSe crystal (approximately 95 mJ/cm^2) and the challenging output energy scaling of a 3 μm nanosecond pump laser. To enhance the output energy, we developed an additional amplification stage.

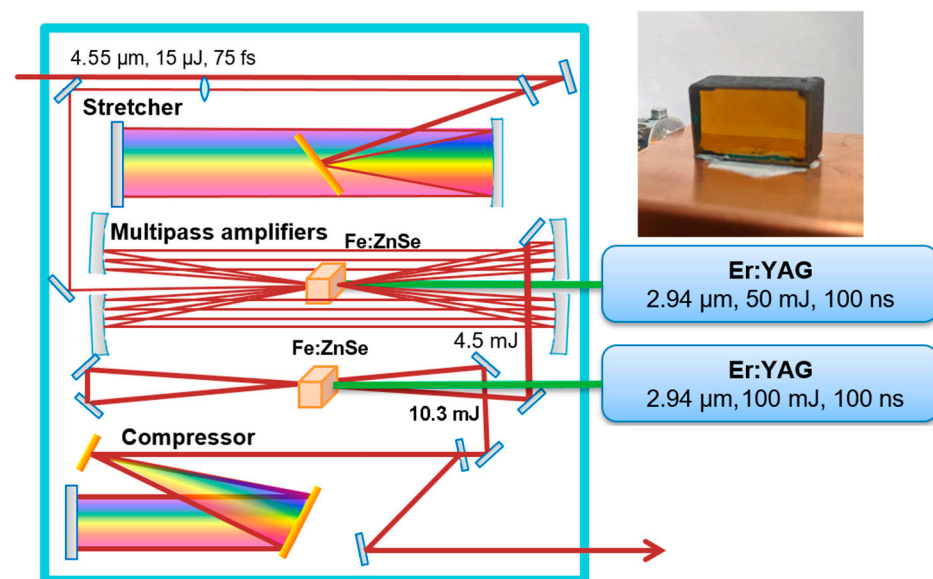


Figure 1. The layout of the Fe:ZnSe chirped pulse amplification laser system with two stages of multi-pass amplification. A photo of Fe:ZnSe, placed in the second amplifier stage, is presented in the inset.

The first mid-IR multi-pass amplifier design required reaching the maximum energy extraction from it with a minimum number of passes. This scheme was based on four curved mirrors, with caustic control provided by CaF_2 lenses to ensure further collimated beam propagation after the amplifier. The output energy of 4.5 mJ was achieved after this stage, which was in a good correspondence with our calculations of gain dynamics according to the Franz–Nodvik theory with nonradiative losses to estimate the stored energy.

In order to increase the output energy, we designed a second amplifier with two passes through the gain media. The pump beam was focused on a spot with a diameter of about

4 mm (intensity $1/e^2$) to achieve an optimal pump fluence of about 0.8 J/cm^2 and a seed fluence comparable to the saturation fluence ($\sim 30 \text{ mJ/cm}^2$) with the same beam size.

For pumping, a nanosecond master oscillator power amplifier (MOPA) system based on Er:YAG crystals ($2.94 \text{ }\mu\text{m}$) was developed in our laboratory and utilized. The choice of the crystal is attributed to the high absorption coefficient of the Fe:ZnSe crystal at this wavelength and the favorable thermo-optical properties of Er:YAG, which results in the high beam quality of the output laser radiation. Additionally, electro-optical Q-switching enables low-jitter timing with precise delay tuning between the pump and $4 \text{ }\mu\text{m}$ seed pulses. The developed MOPA system consisted of two amplification stages that provided energy values of up to 100 mJ . The development of a pump laser with several cascades of amplification stages is challenging due to the relatively small gain (of about 1.4 for 100 J flashlamp pump energy) of the Er:YAG crystal and the beam distortions introduced by the thermal lens. Moreover, the output energy from the oscillator is limited by the damage threshold of the optical elements, particularly the Q-switches. However, this limitation can be overcome with the use of novel durable electro-optic materials transparent in the mid-IR range [25,26].

For broadband amplification, a Fe:ZnSe anti-reflection coated polycrystalline element with dimensions of $10.5 \times 17 \times 8 \text{ mm}^3$ and an average concentration of $1.3 \times 10^{18} \text{ cm}^{-3}$ was utilized. It was produced by doping the ZnSe substrate from the iron film using the process of hot isostatic pressing (HIP) at the Devyatikh Institute of Chemistry of High-Purity Substances of the Russian Academy of Sciences (ICHPS RAS). The growth methods for Fe:ZnSe crystals are well-established, allowing for various doping profiles, such as homogeneous concurrent-doping technology [27] or a doping gradient via a simpler and more cost-effective post-growth doping method [28]. This approach enables the control of the gain and the positioning of the gain spectrum. Previous research has indicated that a high level of doping results in concentration quenching, and the reduction in the lifetime of the upper laser level, due to the short lifetime of such crystals at room temperature, requires the nanosecond duration of the laser pumping pulses [19]. To prevent the crystal from overheating under intense pumping, in this paper, it was mounted onto a copper heatsink cooled with water at $10 \text{ }^\circ\text{C}$.

After the second amplifier, an output energy of up to about 10 mJ was achieved in the Gaussian-like laser beam (see Figure 2). In the case of high-gain laser media, the problem of transverse parasitic lasing is relevant, as it depletes the energy storage and decreases the gain coefficient for an amplified laser pulse [29]. To address this, the crystal's side facets can be coated with an absorbing substance, such as black ink, to minimize reflection from the walls when the refractive indices are matched, thus reducing the feedback. In our case, we applied a black matte paint, prolonging the time delay between the pumping and seed pulses under the conditions of high gain in the amplifier and diminishing the requirement for crystal orientation, although no significant gain increase was observed. Our future investigations will explore alternative compositions, particularly those containing soot, to enhance refractive index matching.

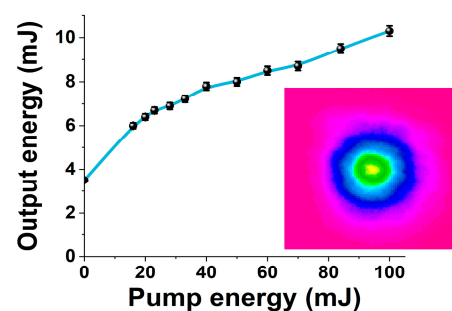


Figure 2. Output pulse energy from the second multi-pass amplifier stage versus pump energy. The intensity profile at the maximum pumping energy is depicted in the inset.

The utilization of multiple amplification stages at a moderate pump fluence level represents a promising approach for scaling the output energy while mitigating issues such as amplified spontaneous emission (ASE), concentration quenching in the active element, and the decrease in the laser beam quality. This strategy is well-suited for achieving mJ level output energy in chirped pulse amplification (CPA) systems with a mode-locked master oscillator or parametric frontend. These systems are often essential for high-field physics research and the generation of terahertz (THz) radiation using mid-IR sources [30,31].

3. Tunability and Spectral Synthesis

It is a natural desire to fill the gap between the gain bands of the Cr:ZnS/Se and Fe:ZnSe crystals with central generation wavelengths of 2.4 μm and 4.4 μm , respectively, to shift to the region of large wavelengths, and to obtain pulses as short as possible from the source without the need of nonlinear post-compression, and based on this, to develop a wide-range laser system covering most of the mid-IR spectral region.

In the first case, a promising active media candidate is a Fe:ZnS crystal with a gain bandwidth centered at 3.7 μm . Previous studies have showcased narrowband pulsed generation based on this gain medium [32]. While the Cr:ZnS gain spectrum shift is insignificant compared to that of Cr:ZnSe, it is noticeable in iron-ion-containing hosts. However, lasing in such a media is hindered by their short lifetime at room temperature, a characteristic shared with other Fe-doped active media, and requires cryogenic cooling for energy storage. At room temperature, the lifetime is estimated to be 50 ns, increasing to 1–2 μs at the liquid nitrogen temperature [33]. Nonetheless, this crystal supports broadband tuning from 3.4 to 4.2 μm [8], even at such low temperatures, and is expected to amplify broadband pulses.

The experimental setup for broadband amplification using the Fe:ZnS crystal is depicted in Figure 3a. According to the literature data, the peak gain cross-section for this crystal is located near the wavelength of 3.7 μm , while the absorption band is approximately at 3.0 μm [32]. The seeding source comprised an optical parametric amplifier (OPA) broadly tunable in the mid-IR range, generating a pulse energy of about 5 μJ at a central wavelength of 3.7 μm . The pump beam was focused on the crystal facet with a fluence of about 0.8–1.0 J/cm^2 —optimal for other chalcogenides doped with iron ions and at a safe level relative to the crystal's damage threshold. The active element was housed in a cryostat with windows transparent in the mid-IR range and cooled with liquid nitrogen. Fe:ZnS samples, also manufactured at ICHPS RAS, with a thickness of 3 mm were utilized. The measurement of pump radiation absorption, adjusted for Fresnel reflection, revealed an absorption coefficient of 3.6 cm^{-1} .

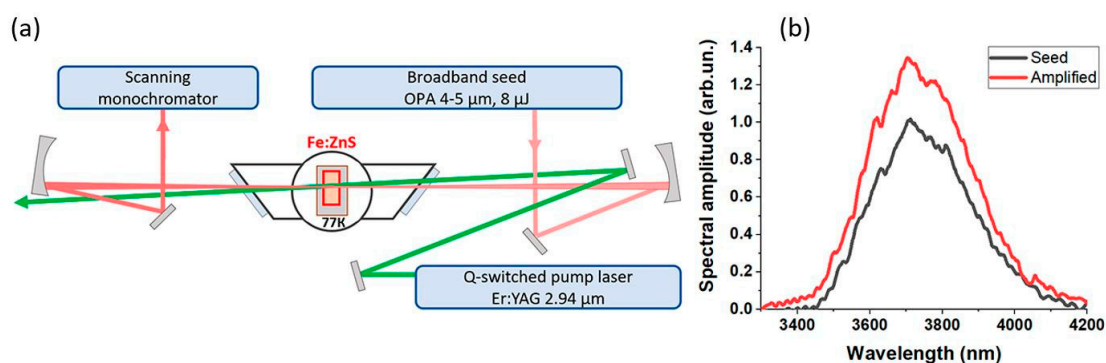


Figure 3. Experimental setup (a) and transformation of the broadband seed spectrum (b) under amplification using a cryogenically cooled Fe:ZnS crystal.

A scanning monochromator with a pyroelectric detector was utilized to record the spectrum transformation during amplification (Figure 3b). The gain across the entire spectrum was about 1.25. Single-pass amplification maintained the spectrum's original width, suggesting the potential for scaling energy in a multi-pass amplification scheme. Despite

the high absorption coefficient, the gain remained relatively low, although papers dedicated to lasing in such a crystal claim high efficiency. This is likely due to the predominant role of ASE (amplified spontaneous emission) in the amplification process, resulting in the majority of the stored energy being expended on spontaneous transitions, with the amplified signal removing only a small portion of the inversion. Unfortunately, this phenomenon is typical for chalcogenide crystals, and a finer control of pumping and seeding fluences is required. Probably, the amplification efficiency can be increased with a better matching of the pump wavelength to the absorption spectrum and a shorter pulse duration, obtained, for example, with Er:YLF lasers [34].

Fe:CdSe and Fe:CdTe crystals have gain bands located in a longer wavelength range compared to Fe:ZnSe [13,35,36]. Fe:CdSe also requires cryogenic cooling to increase the lifetime and gain cross-section. On the other hand, Fe:CdTe does not, but its shifted absorption band makes pumping with 3 μm laser sources inefficient. Scientific efforts have been focused on enhancing the efficiency of laser generation, suppressing spontaneous luminescence amplification, broadening the amplification spectrum, and increasing absorption from the available pump sources.

Spectral synthesis offers an elegant approach to broadening the amplification spectrum in composite laser media. This method involves a cascade amplification of a broadband seeding pulse in various laser media, where each medium is not individually able to support its entire width. This method has primarily been developed for parametric laser sources. Narrowband generation in a combined active medium based on chalcogenides doped with chromium ions has been studied in the gain-switching mode in a tunable cavity [37]. By combining Cr:ZnSe and Cr:CdSe crystals, it was possible to expand the tuning spectrum compared to an oscillator based on each of the crystals separately.

In the context of the discussed work, this investigation focused on the operation of a broadband laser pulse amplifier in the range of 4–5 μm based on chalcogenide crystals doped with iron ions. Previous studies have shown that the Fe:ZnSe crystal is capable of amplifying broadband laser pulses in the spectral band from 3.8 μm to 4.8 μm . However, with longer wavelength seeding, instead of amplification, the stored energy is converted into amplified spontaneous emission in the region of 4.3–4.4 μm , where the gain cross-section reaches its maximum. It is possible to extend the long-wavelength part of the spectrum with the help of amplification in the Fe:CdSe crystal, which has a gain band located at 4.4–5.5 μm , cut by absorption in the active element itself at shorter wavelengths and by absorption of atmospheric moisture at longer wavelengths.

The experimental setup is illustrated in Figure 4a. Similar to previous experiments, an optical parametric amplifier (OPA), tunable at 4–5 μm and with a spectral width of up to 600 nm (FWHM), served as the seeding source. An Er:YAG nanosecond laser (2.94 μm , 25 mJ, and 110 ns) was employed to simultaneously pump both crystals. The Fe:CdSe crystal was grown from the vapor phase on a single-crystal seed by using concurrent-doping technology, developed in the Lebedev Physical Institute of the Russian Academy of Sciences. Crystals grown using this technique possess high structural quality, optical homogeneity, and as a result, low intrinsic losses. It was cryogenically cooled to the temperature of liquid nitrogen to enhance its lifetime. The Fe:ZnSe crystal was installed inside the cryostat, but not on a cold finger, at a distance of approximately 0.5 cm from the Fe:CdSe crystal.

The pumping and seeding beams, placed at a small angle from each other, were initially directed to the Fe:CdSe crystal, as most of the short-wave radiation amplified in Fe:ZnSe would otherwise be absorbed in the Fe:CdSe crystal. The Fe:CdSe crystal exhibited approximately 25% transmission at the pump wavelength, owing to its cooling to the temperature of liquid nitrogen.

The transformation of the pulse spectrum was examined for seeding pulses centered at 4.5 μm (Figure 4b). The dip in the vicinity of 4.3 μm was attributed to CO₂ absorption and can be entirely mitigated by subjecting the setup to vacuum conditions or by substituting it with a noble gas, which would preserve the bandwidth of the amplified pulse. The Fe:CdSe

crystal contributed to the amplification of the long-wave part of the spectrum, while Fe:ZnSe facilitated the amplification of the spectrum in the short-wave region. Consequently, the combination of these chalcogenide crystals doped with iron ions in the amplifier offers the potential to support more extensive broadband amplification than a single active medium.

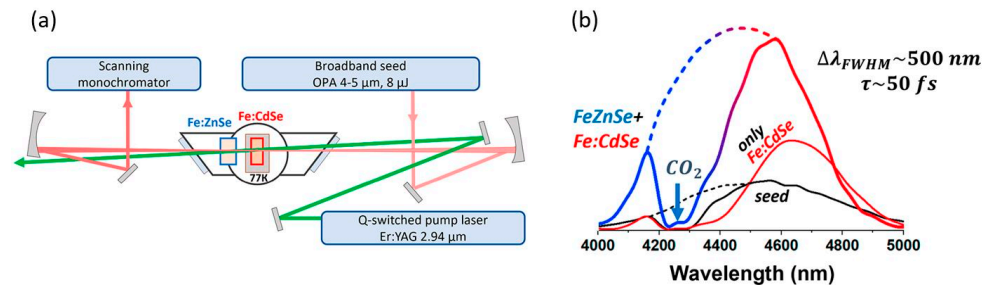


Figure 4. Experimental setup (a) and transformation of the broadband seed spectrum (b) under amplification in a set of Fe-doped chalcogenide crystals: room-temperature Fe:ZnSe and cryogenically cooled Fe:CdSe.

4. Properties of Single-Wall Nanotubes in the mid-IR Range

The study focused on the properties of the nonlinear optical response of single-wall nanotubes (SWNTs) when subjected to femtosecond mid-IR laser pulses. The research involved measuring the SWNTs’ nonlinear absorption and the nonlinear component of the refractive index. Three types of carbon nanotube samples in the form of thin (~100 nm) films were synthesized at the Skolkovo Institute of Science and Technology using aerosol production, primarily differing in diameter. The absorption spectra of the samples, measured with the spectrophotometer, is depicted in Figure 5. The absorption peaks were observed near the wavelengths of 1.8 μm and 2.8 μm, corresponding to the nanotube radii of 1.2 nm and 2.0 nm, respectively. Certain samples were densified, leading to a reduction in their thickness by approximately half.

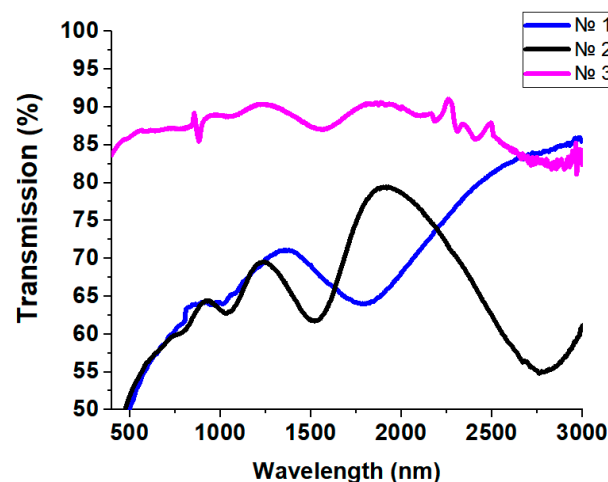


Figure 5. Absorption spectrum of the manufactured samples of single-walled carbon nanotubes, measured using a spectrophotometer.

Previously, the SWNT properties were evaluated in a Fe:ZnSe ultrashort laser pulse oscillator by substituting graphene for the mode-locking process, as developed by our group. For effective absorption at wavelengths of approximately 4.1–4.4 μm, the nanotube diameter should be within the range of 2.7–2.9 nm. However, fabricating SWNTs with such a large diameter is challenging, as it requires catalytic particles of a substantial size, which increases the likelihood of multi-walled nanotube growth. In the study in reference [38], nanotubes with a diameter of 2.2 nm were employed to achieve the mode-locking regime in

the Cr:ZnSe oscillator at a wavelength of 2.4 μm , yielding 49 fs pulses. Nevertheless, reports also exist of mode-locking in the Cr:ZnSe laser [39] using nanotubes with a considerably smaller diameter, producing 61 fs pulses at a wavelength of 2.35 μm . Carbon nanomaterials exhibit a lower saturation intensity and a higher modulation depth at longer wavelengths, rendering them advantageous as saturable absorbers.

The ability of carbon nanotubes to achieve the mode-locking regime of laser generation inside the mid-IR laser cavity due to saturated absorption has been investigated in a Fe:ZnSe laser. In the setup described in reference [22], SWNTs deposited on a BaF₂ wafer were utilized instead of graphene, resulting in the generation of a pulse train with SWNT samples at the power of approximately 200 mW. For comparison, with graphene, the laser radiation power was 415 mW under the same setup parameters. SWNTs are anticipated to demonstrate saturated absorption, which distinguishes continuous generation from mode-locking with significant unsaturated losses compared to graphene. The pulse duration was measured using the frequency-resolved optical gating (FROG) technique based on second-harmonic generation in a GaSe crystal, revealing a pulse duration of 660 fs (Figure 6), likely associated with the response time in carbon nanotubes when they act as a fast saturable absorber.

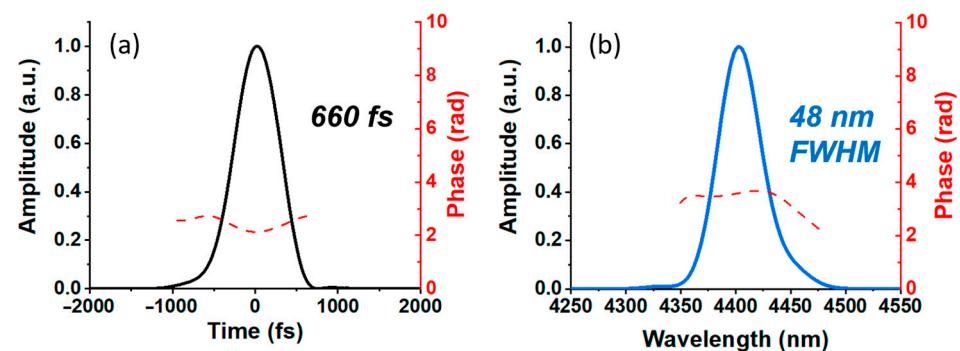


Figure 6. Pulse envelope (a) and spectrum (b) retrieved using the FROG technique from the Fe:ZnSe oscillator in the mode-locking regime based on saturable absorption in single-wall nanotubes. The red dashed line depicts the temporal phase.

This research conducted Z-scan measurements to comprehensively characterize the optical properties of SWNTs in the infrared range. These measurements were performed with an open aperture to evaluate saturated absorption and with a closed aperture to determine the real part of the nonlinear refractive index. An optical parametric amplifier (OPA) with specific parameters was used as the pumping source. The laser beam, with a central wavelength of 4.5 μm , was focused by a lens into a diameter of 160 μm , providing an intensity of 0.5 TW/cm² in the focus. An intensity of about 100 GW/cm² was chosen for the operation, aiming to prevent the breakdown of the SWNTs. The Z-scan measurements with an open aperture showed an increase in saturation in the SWNTs, as opposed to bleaching, with a significant absorption dip of up to 40% (Figure 7a). When conducting Z-scan measurements with a closed aperture (Figure 7b), the recorded absorption dip blurs the signal, likely due to photoinduced absorption. The decrease in transmission is attributed to this phenomenon. In reference [40], the dynamics and the properties of absorption in nanotubes were studied using the degenerate pump–probe technique in a wide spectral range. Thus, in nanotubes with an absorption peak at 1800 nm, the transition to photoinduced absorption occurred already at a wavelength of 2100 nm. This transition is explained by the competition between the Pauli exclusion principle and the renormalization of the bandgap [41].

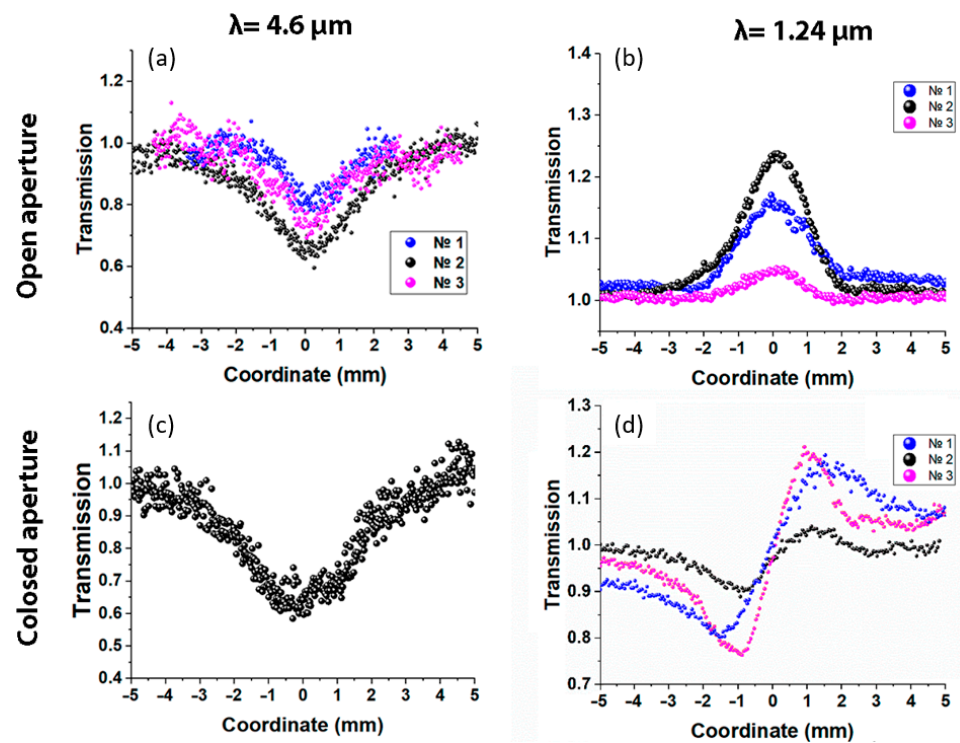


Figure 7. Transmission of the SWNT samples depending on the coordinates obtained in the Z-scan with open (a,b) and closed (c,d) apertures at the wavelengths of 4.6 μm (left column) and 1.24 μm (right column).

We conducted similar experiments with femtosecond pulses at a wavelength of 1.24 μm from a Cr: Forsterite laser (1 μJ and 100 fs) (Figure 7c,d). In this case, absorption saturation was observed in measurements with an open aperture. The saturation constant was determined by a standard method based on the amplitude of the increase in the transmission and pumping pulse parameters and ranged from $0.8 \times 10^8 \text{ cm/W}$ to $3.1 \times 10^8 \text{ cm/W}$ for different samples. The value of the nonlinear refractive index n_2 obtained from the open aperture measurements turned out to be negative and ranged from $-0.27 \times 10^{-12} \text{ cm}^2/\text{W}$ to $-0.98 \times 10^{-12} \text{ cm}^2/\text{W}$.

Low-dimensional carbon materials that demonstrate saturated absorption play a crucial role in facilitating the mode-locking process in a wide array of near- and mid-infrared solid-state and fiber lasers. This phenomenon effectively suppresses low-intensity radiation within the laser cavity, facilitating the formation of ultrashort laser pulses. The ability to control the properties of these absorbers is particularly significant for lasers utilizing media with ASE, such as those employing iron-ion-doped chalcogenides. Consequently, the carbon nanotubes' saturated absorption has the potential to serve as the foundation for developing contrast cleaners for high-power laser systems. To achieve this, the characteristics of the absorber have to be matched to the laser radiation properties in terms of the absorption spectrum and damage threshold. The study and effective management of the properties of carbon nanotubes can be facilitated by utilizing mid-infrared laser sources based on the chalcogenides themselves, providing the necessary flexibility and a margin for the corresponding output parameters.

5. Discussion

In this paper, novel approaches were considered to expand the spectral band covered by active media based on chalcogenides doped with iron ions. The example of a CPA laser system based on a Fe:ZnSe crystal showed that the prospect of reaching the terawatt power level entails an increase in the number of amplifiers. The superior properties of the Fe:ZnSe crystal provide such an opportunity due to energy scalable 3- μm nanosecond pumping

sources. On the other hand, the high gain also prevents efficient energy extraction due to transverse emission processes, which imposes a requirement for the precise control of the sizes of the pump and the seed beams.

Another promising active medium from the group of iron-doped selenide crystals for the broadband amplification of mid-IR laser pulses is Fe:ZnS. The corresponding experiments showed no spectral width narrowing of the seed laser pulse (~300 nm (FWHM)) centered at 3.7 μm . A small gain coefficient, compared to that of Fe:ZnSe, can probably be increased at a more suitable pumping wavelength, for example, in a Er:YLF laser operating at 2.67 μm , which offers the prospect of its use in multi-pass amplification schemes. The spectral synthesis scheme allows one to cover a wider spectral band during the amplification process, and in general, it is not limited to just two active elements. Despite the fact that a common feature of the media studied in this paper is the possibility of pumping by 3 μm lasers, an obstacle is the overlap of their gain and absorption bands. However, this can be resolved in schemes where the seed is split into several channels in different spectral ranges. Then, each part is directed to the appropriate active element with an appropriate gain spectrum. After that, all channels are combined on specific spectrally selective optics. In this case, it is possible to obtain even more broadband laser pulses.

Experiments on the properties of carbon nanotubes have shown the importance of controlling their parameters (in particular, the diameter) to characterize their properties in the mid-IR region. The mechanism of mode-locking in the Fe:ZnSe laser cavity in the absence of saturating absorption remains unclear, which, however, makes such objects even more interesting for the development of the component base for mid-IR photonics.

6. Conclusions

Powerful mid-IR laser systems are relevant in many high-peak power-demanding applications, requiring the precise control of the laser characteristics in terms of output energy and pulse duration. Gain elements based on chalcogenides doped with iron ions, owing to their exceptional amplifying properties and vibronic nature, offer a broad gain, enabling the convenient manipulation of these parameters. In chalcogenide-based chirped pulse amplification (CPA) systems, the output energy can be scaled using additional amplifier stages in relatively simple configurations with several passes. Furthermore, the spectral properties can be adjusted by selecting an appropriate crystal host. For instance, the Fe:ZnS crystal supports broadband amplification in the vicinity of 3.7 μm , while a spectral synthesis scheme, particularly based on Fe:ZnSe and Fe:ZnS crystals, facilitates the broadening of the gain bandwidth for the broadband seed pulse.

Low-dimensional carbon materials show promise for the development of photonic components in the mid-IR spectral range. Carbon nanotubes, for example, can be utilized to implement the mode-locking regime in the Fe:ZnSe laser cavity, offering potential for the development of novel photonic devices. However, the study of their properties requires enhanced technological flexibility in controlling the size of the nanotubes.

Author Contributions: Conceptualization, methodology, resources, supervision, project administration, funding acquisition, investigation, writing—review and editing, F.P.; investigation, writing—original draft preparation, A.P. All authors have read and agreed to the published version of the manuscript.

Funding: This research was funded by the Russian Science Foundation (project No. 20-19-00148 for THz radiation approaches) and by the Russian Foundation for Basic Research (project No. 21-52-50005 for the investigation of carbon nanotubes' nonlinear properties in the mid-IR range). The equipment used in this work was purchased with the support of the Program for the Development of Moscow State University and the National Project "Science and Universities".

Data Availability Statement: Data can be provided upon request.

Acknowledgments: The authors thank Y. Gladush from Skoltech for providing the single-wall nanotubes investigated in the present study and S.S. Balabanov, D.V. Savin, V.B. Ikonnikov, and E.M. Gavrishchuk for providing the Fe:ZnSe polycrystalline samples.

Conflicts of Interest: The authors declare no conflict of interest.

References

1. Pushkin, A.; Migal, E.; Suleimanova, D.; Mareev, E.; Potemkin, F. High-Power Solid-State Near- and Mid-IR Ultrafast Laser Sources for Strong-Field Science. *Photonics* **2022**, *9*, 90. [[CrossRef](#)]
2. Adams, J.J.; Bibeau, C.; Page, R.H.; Krol, D.M.; Furu, L.H.; Payne, S. 4.0–4.5- μm Lasing of Fe:ZnSe below 180 K, a New Mid-Infrared Laser Material. *Opt. Lett.* **1999**, *24*, 1720–1722. [[CrossRef](#)] [[PubMed](#)]
3. Popmintchev, T.; Chen, M.-C.; Popmintchev, D.; Arpin, P.; Brown, S.; Ališauskas, S.; Andriukaitis, G.; Balčiunas, T.; Mücke, O.D.; Pugzlys, A.; et al. Bright Coherent Ultrahigh Harmonics in the KeV X-Ray Regime from Mid-Infrared Femtosecond Lasers. *Science* **2012**, *336*, 1287–1291. [[CrossRef](#)] [[PubMed](#)]
4. Rumiantsev, B.V.; Mikheev, K.E.; Pushkin, A.V.; Migal, E.A.; Stremoukhov, S.Y.; Potemkin, F.V. Optical Harmonics Generation under the Interaction of Intense (up to 10^{14} W/cm²) Mid-Infrared Femtosecond Laser Radiation of a Fe:ZnSe Laser System with a Dense Laminar Gas Jet. *JETP Lett.* **2022**, *115*, 390–395. [[CrossRef](#)]
5. Yakovlev, V.S.; Ivanov, M.; Krausz, F. Enhanced Phase-Matching for Generation of Soft X-Ray Harmonics and Attosecond Pulses in Atomic Gases. *Opt. Express* **2007**, *15*, 15351. [[CrossRef](#)]
6. Castelvetti, D.; Sanderson, K. Physicists Who Built Ultrafast ‘Attosecond’ Lasers Win Nobel Prize. *Nature* **2023**, *622*, 225–227. [[CrossRef](#)]
7. Fedorov, V.V.; Mirov, S.B.; Gallian, A.; Badikov, D.V.; Frolov, M.P.; Korostelin, Y.V.; Kozlovsky, V.I.; Landman, A.I.; Podmar'kov, Y.P.; Akimov, V.A.; et al. 3.77–5.05- μm Tunable Solid-State Lasers Based on Fe²⁺-Doped ZnSe Crystals Operating at Low and Room Temperatures. *IEEE J. Quantum Electron.* **2006**, *42*, 907–917. [[CrossRef](#)]
8. Frolov, M.P.; Korostelin, Y.V.; Kozlovsky, V.I.; Podmar'kov, Y.P.; Savinova, S.A.; Skasyrsky, Y.K. 3 J Pulsed Fe:ZnS Laser Tunable from 3.44 to 4.19 μm . *Laser Phys. Lett.* **2015**, *12*, 055001. [[CrossRef](#)]
9. Antipov, O.; Novikov, A.; Larin, S.; Obronov, I. Highly Efficient 2 μm CW and Q-Switched Tm³⁺:Lu₂O₃ Ceramics Lasers in-Band Pumped by a Raman-Shifted Erbium Fiber Laser at 1670 nm. *Opt. Lett.* **2016**, *41*, 2298. [[CrossRef](#)]
10. Švejkar, R.; Šulc, J.; Jelínková, H. Er-Doped Crystalline Active Media for ~3 μm Diode-Pumped Lasers. *Prog. Quantum Electron.* **2020**, *74*, 100276. [[CrossRef](#)]
11. Migal, E.; Pushkin, A.; Bravy, B.; Gordienko, V.; Minaev, N.; Sirotkin, A.; Potemkin, F. 3.5-mJ 150-fs Fe:ZnSe Hybrid Mid-IR Femtosecond Laser at 4.4 μm for Driving Extreme Nonlinear Optics. *Opt. Lett.* **2019**, *44*, 2550. [[CrossRef](#)]
12. Mirov, S.; Moskalev, I.; Vasilyev, S.; Smolski, V.; Fedorov, V.; Martyshkin, D.; Peppers, J.; Mirov, M.; Dergachev, A.; Gapontsev, V. Frontiers of Mid-IR Lasers Based on Transition Metal Doped Chalcogenides. *IEEE J. Sel. Top. Quantum Electron.* **2018**, *24*, 1601829. [[CrossRef](#)]
13. Pushkin, A.; Potemkin, F. High-Gain Broadband Laser Amplification of Mid-IR Pulses in Fe:ZnSe Crystal at 5 μm with Millijoule Output Energy and Multigigawatt Peak Power. *Opt. Lett.* **2022**, *47*, 5762. [[CrossRef](#)]
14. Leshchenko, V.E.; Talbert, B.K.; Lai, Y.H.; Li, S.; Tang, Y.; Hageman, S.J.; Smith, G.; Agostini, P.; DiMauro, L.F.; Blaga, C.I. High-Power Few-Cycle Cr:ZnSe Mid-Infrared Source for Attosecond Soft X-ray Physics. *Optica* **2020**, *7*, 981. [[CrossRef](#)]
15. Wu, Y.; Zhou, F.; Larsen, E.W.; Zhuang, F.; Yin, Y.; Chang, Z. Generation of Few-Cycle Multi-Millijoule 2.5 μm Pulses from a Single-Stage Cr²⁺:ZnSe Amplifier. *Sci. Rep.* **2020**, *10*, 7775. [[CrossRef](#)]
16. Rudenkov, A.; Kalashnikov, V.L.; Sorokin, E.; Demesh, M.; Sorokina, I.T. High Peak Power and Energy Scaling in the Mid-IR Chirped-Pulse Oscillator-Amplifier Laser Systems. *Opt. Express* **2023**, *31*, 17820. [[CrossRef](#)]
17. Marra, Z.A.; Wu, Y.; Zhou, F.; Chang, Z. Cryogenically Cooled Fe:ZnSe-Based Chirped Pulse Amplifier at 4.07 μm . *Opt. Express* **2023**, *31*, 13447. [[CrossRef](#)]
18. Li, E.; Uehara, H.; Tokita, S.; Yao, W.; Yasuhara, R. A Hybrid Quantum Cascade Laser/Fe:ZnSe Amplifier System for Power Scaling of CW Lasers at 4.0–4.6 μm . *Opt. Laser Technol.* **2023**, *157*, 108783. [[CrossRef](#)]
19. Migal, E.A.; Balabanov, S.S.; Savin, D.V.; Ikonnikov, V.B.; Gavrishchuk, E.M.; Potemkin, F.V. Amplification Properties of Polycrystalline Fe:ZnSe Crystals for High Power Femtosecond Mid-IR Laser Systems. *Opt. Mater.* **2021**, *111*, 110640. [[CrossRef](#)]
20. Krauss, G.; Lohss, S.; Hanke, T.; Sell, A.; Eggert, S.; Huber, R.; Leitenstorfer, A. Synthesis of a Single Cycle of Light with Compact Erbium-Doped Fibre Technology. *Nat. Photonics* **2010**, *4*, 33–36. [[CrossRef](#)]
21. Cho, W.B.; Yim, J.H.; Choi, S.Y.; Lee, S.; Schmidt, A.; Steinmeyer, G.; Griebner, U.; Petrov, V.; Yeom, D.-I.; Kim, K.; et al. Boosting the Non Linear Optical Response of Carbon Nanotube Saturable Absorbers for Broadband Mode-Locking of Bulk Lasers. *Adv. Funct. Mater.* **2010**, *20*, 1937–1943. [[CrossRef](#)]
22. Pushkin, A.V.; Migal, E.A.; Tokita, S.; Korostelin, Y.V.; Potemkin, F.V. Femtosecond Graphene Mode-Locked Fe:ZnSe Laser at 4.4 μm . *Opt. Lett.* **2020**, *45*, 738. [[CrossRef](#)]
23. Frolov, M.P.; Korostelin, Y.V.; Kozlovsky, V.I.; Podmar'kov, Y.P.; Skasyrsky, Y.K. Efficient 10-J Pulsed Fe:ZnSe Laser at 4100 nm. In Proceedings of the 2016 International Conference Laser Optics (LO), St. Petersburg, Russia, 24 June–1 July 2016; Volume 247, p. R110. [[CrossRef](#)]
24. Velikanov, S.D.; Gavrishchuk, E.M.; Zaretsky, N.A.; Zakhryapa, A.V.; Ikonnikov, V.B.; Kazantsev, S.Y.; Kononov, I.G.; Maneshkin, A.A.; Mashkovskii, D.A.; Saltykov, E.V.; et al. Repetitively Pulsed Fe : ZnSe Laser with an Average Output Power of 20 W at Room Temperature of the Polycrystalline Active Element. *Quantum Electron.* **2017**, *47*, 303–307. [[CrossRef](#)]
25. Zhang, H.; Li, Y.; Wu, Q. 2.79 μm LGS Electro-Optical Q-Switched Er, Cr: YSGG Laser. *Opt. Commun.* **2022**, *503*, 127448. [[CrossRef](#)]

26. Yushkov, K.B.; Chizhikov, A.I.; Naumenko, N.F.; Molchanov, V.; Pavlyuk, A.; Makarevskaya, E.V.; Zakharov, N.G. KYW Crystal as a New Material for Acousto-Optical Q-Switches. In Proceedings of the Components and Packaging for Laser Systems V, San Francisco, CA, USA, 4–6 February 2019; p. 1089913.
27. Korostelin, Y.V.; Kozlovsky, V.I. Vapour Growth of II–VI Solid Solution Single Crystals by Contact-Free Technique. *J. Alloys Compd.* **2004**, *371*, 25–30. [[CrossRef](#)]
28. Avetisov, R.I.; Balabanov, S.S.; Firsov, K.N.; Gavrishchuk, E.M.; Gladilin, A.A.; Ikonnikov, V.B.; Kalinushkin, V.P.; Kazantsev, S.Y.; Kononov, I.G.; Zykova, M.P.; et al. Hot-Pressed Production and Laser Properties of ZnSe:Fe²⁺. *J. Cryst. Growth* **2018**, *491*, 36–41. [[CrossRef](#)]
29. Dormidonov, A.E.; Firsov, K.N.; Gavrishchuk, E.M.; Ikonnikov, V.B.; Kononov, I.G.; Kurashkin, S.V.; Podlesnykh, S.V.; Savin, D.V. Suppression of Transverse Parasitic Oscillation in Fe:ZnSe and Fe:ZnS Lasers Based on Polycrystalline Active Elements: A Review. *Phys. Wave Phenom.* **2020**, *28*, 222–230. [[CrossRef](#)]
30. Koulouklidis, A.D.; Gollner, C.; Shumakova, V.; Fedorov, V.Y.; Pugžlys, A.; Baltuška, A.; Tzortzakis, S. Observation of Extremely Efficient Terahertz Generation from Mid-Infrared Two-Color Laser Filaments. *Nat. Commun.* **2020**, *11*, 292. [[CrossRef](#)]
31. Gollner, C.; Shalaby, M.; Brodeur, C.; Astrauskas, I.; Jutas, R.; Constable, E.; Bergen, L.; Baltuška, A.; Pugžlys, A. Highly Efficient THz Generation by Optical Rectification of Mid-IR Pulses in DAST. *APL Photonics* **2021**, *6*, 046105. [[CrossRef](#)]
32. Kozlovsky, V.I.; Akimov, V.A.; Frolov, M.P.; Korostelin, Y.V.; Landman, A.I.; Martovitsky, V.P.; Mislavskii, V.V.; Podmar'kov, Y.P.; Skasyrsky, Y.K.; Voronov, A.A. Room-Temperature Tunable Mid-Infrared Lasers on Transition-Metal Doped II–VI Compound Crystals Grown from Vapor Phase. *Phys. Status Solidi Basic Res.* **2010**, *247*, 1553–1556. [[CrossRef](#)]
33. Myoung, N.; Fedorov, V.V.; Mirov, S.B.; Wenger, L.E. Temperature and Concentration Quenching of Mid-IR Photoluminescence in Iron Doped ZnSe and ZnS Laser Crystals. *J. Lumin.* **2012**, *132*, 600–606. [[CrossRef](#)]
34. Messner, M.; Heinrich, A.; Hagen, C.; Unterrainer, K. Acousto-Optically Q-Switched Diode Side-Pumped Er:YLF Laser Generating 50 kW Peak Power in 70 ns Pulses. In *Solid State Lasers XXVIII: Technology and Devices, San Francisco, CA, USA, 5–7 February 2019*; Clarkson, W.A., Shori, R.K., Eds.; SPIE: Cergy-Pontoise, France, 2019; p. 6. [[CrossRef](#)]
35. Kozlovsky, V.I.; Korostelin, Y.V.; Podmar'kov, Y.P.; Skasyrsky, Y.K.; Frolov, M.P. Middle Infrared Fe²⁺: ZnS, Fe²⁺: ZnSe and Cr²⁺: CdSe Lasers: New Results. *J. Phys. Conf. Ser.* **2016**, *740*, 012006. [[CrossRef](#)]
36. Frolov, M.P.; Korostelin, Y.V.; Kozlovsky, V.I.; Leonov, S.O.; Skasyrsky, Y.K. Tunable in the Range of 4.5–6.8 μm Room Temperature Single-Crystal Fe: CdTe Laser Pumped by Fe: ZnSe Laser. *Opt. Express* **2020**, *28*, 17449. [[CrossRef](#)] [[PubMed](#)]
37. Aikawa, S.; Yumoto, M.; Saitoh, T.; Wada, S. Mid-Infrared Tunable Pulsed Laser Based on Cr²⁺-Doped II–VI Chalcogenide. *J. Cryst. Growth* **2021**, *575*, 126341. [[CrossRef](#)]
38. Okazaki, D.; Arai, H.; Anisimov, A.; Kauppinen, E.I.; Chiashi, S.; Maruyama, S.; Saito, N.; Ashihara, S. Self-Starting Mode-Locked Cr:ZnS Laser Using Single-Walled Carbon Nanotubes with Resonant Absorption at 2.4 μm. *Opt. Lett.* **2019**, *44*, 1750. [[CrossRef](#)]
39. Tolstik, N.; Okhotnikov, O.; Sorokin, E.; Sorokina, I.T. Femtosecond Cr:ZnS Laser at 2.35 μm Mode-Locked by Carbon Nanotubes. In Proceedings of the Solid State Lasers XXIII Technology and Devices, San Francisco, Ca, USA, 2–4 February 2014; Volume 8959, p. 89591A. [[CrossRef](#)]
40. Xu, S.; Wang, F.; Zhu, C.; Meng, Y.; Liu, Y.; Liu, W.; Tang, J.; Liu, K.; Hu, G.; Howe, R.C.T.; et al. Ultrafast Nonlinear Photoresponse of Single-Wall Carbon Nanotubes: A Broadband Degenerate Investigation. *Nanoscale* **2016**, *8*, 9304–9309. [[CrossRef](#)]
41. Zhu, C.; Liu, Y.; Xu, J.; Nie, Z.; Li, Y.; Xu, Y.; Zhang, R.; Wang, F. Bandgap Renormalization in Single-Wall Carbon Nanotubes. *Sci. Rep.* **2017**, *7*, 11221. [[CrossRef](#)]

Disclaimer/Publisher's Note: The statements, opinions and data contained in all publications are solely those of the individual author(s) and contributor(s) and not of MDPI and/or the editor(s). MDPI and/or the editor(s) disclaim responsibility for any injury to people or property resulting from any ideas, methods, instructions or products referred to in the content.